

Association of a zero-bias anomaly in electron tunneling in $\text{Al}_x\text{Ga}_{1-x}\text{As}$ with the DX defect

R. Magno

Naval Research Laboratory, Washington, D.C. 20375-5000

M. G. Spencer

Naval Research Laboratory, Washington, D.C. 20375-5000

and Department of Electrical Engineering, Howard University, Washington, D.C. 20059

(Received 6 June 1994)

A conductivity peak has been found at zero bias in electron-tunneling measurements on single-barrier $\text{GaAs}/\text{Al}_x\text{Ga}_{1-x}\text{As}/\text{GaAs}$ junctions at 4 K in the dark. The spectral dependence of the quenching of the peak has been measured to extract a photoionization cross section which indicates that the peak is associated with the DX defect. Since zero-bias conductance peaks are a signature of tunneling via paramagnetic defects, the data presented here are consistent with the existence of paramagnetic DX defects.

The DX center found in $\text{Al}_x\text{Ga}_{1-x}\text{As}$, and the GaAs under hydrostatic pressure, has been the focus of much attention because of its metastable nature.^{1,2} Since the DX center is associated with substitutional donors in these materials, a deeper understanding of DX is important to understanding how donors are incorporated into semiconductors. One of the major questions about DX is whether the ground state is charge neutral, DX^0 , with a single electron making it paramagnetic, or whether it is a negative- U center with two electrons, DX^- , where U is the energy required to add the second electron. The negative- U model was proposed in theoretical work by Chadi and Chang, who calculated that the DX ground state is associated with a bond-breaking large lattice relaxation of the Si donor to an interstitial site.³ The inability of electron paramagnetic resonance (EPR),⁴ magnetic circular dichroism absorption,⁵ optically detected electron paramagnetic resonance,⁵ and static magnetic-susceptibility measurements⁶ to detect paramagnetism associated with DX defects has been taken to support the negative- U model. While one magnetic-susceptibility experiment was unable to detect paramagnetism⁶ due to DX defects, another group reported a positive result.⁷ Other evidence in support of the negative- U model has been presented in reports of Hall measurements of GaAs codoped with Ge and Te under hydrostatic pressure,⁸ local vibrational modes of Si-doped GaAs under hydrostatic pressure,⁹ and photoionization of Te-doped $\text{Al}_x\text{Ga}_{1-x}\text{As}$.¹⁰

This paper reports on an electron tunneling spectroscopy experiment on $\text{GaAs}/\text{Al}_x\text{Ga}_{1-x}\text{As}/\text{GaAs}$ junctions with Si spike-doped $\text{Al}_x\text{Ga}_{1-x}\text{As}$ barriers, which demonstrates the existence of paramagnetic DX^0 defects when the DX center is in its ground state. This is a report of the application of this technique, which is totally different from those mentioned above, in the search for paramagnetism associated with the DX defect. An alternate approach like this is important as the absence of a paramagnetic signature in the above-mentioned experiments is not proof that it does not exist. Tunneling measurements are sensitive to the presence of paramagnetic centers,¹¹ though they cannot be used to obtain the detailed structural information EPR can provide. The signature of a paramagnetic center in the barrier of a tunnel junction is a

peak at zero bias in the bias dependence of the conductance, $G(V)$, at liquid-helium temperatures. Past electron-tunneling studies of zero-bias conductance peaks have tested and verified a model¹²⁻¹⁴ that describes the source of the peak as an exchange interaction between paramagnetic impurities in the barrier and the tunneling electrons. The model uses an Anderson Hamiltonian similar to that used to describe localized magnetic moments in nonmagnetic metals.¹⁵ The voltage, temperature, and magnetic-field dependencies of conductance peaks have been reported in a wide variety of tunneling experiments on metal-insulator-metal,^{11,16} and metal-semiconductor junctions.^{11,17,18}

The photoresponse of the DX center in bulk $\text{Al}_x\text{Ga}_{1-x}\text{As}$ is well known, and it is used here to link the zero-bias conductance peak to the DX defect. When bulk $\text{Al}_x\text{Ga}_{1-x}\text{As}$ is exposed to light at liquid-nitrogen temperatures, or lower, the conductivity increases, and the increase persists long after turning the light off. This is associated with the photoionization of a deep DX defect, and the existence of a barrier to recapturing the electron at the DX center.^{1,2} The photoresponse of a tunnel junction with DX defects in the barrier is determined by the decrease in the negative charge in the barrier, as the excited electron will leave the barrier, and by the change in any interactions between the DX defect and the tunneling electrons. The new charge distribution in the barrier needs to be included along with the band gaps and band offsets for GaAs and $\text{Al}_x\text{Ga}_{1-x}\text{As}$ in using Poisson's equation to calculate the shape of the tunnel barrier. The photoionization of DX centers in the $\text{Al}_x\text{Ga}_{1-x}\text{As}$ barriers of resonant-tunneling devices has been shown to produce a persistent increase in the tunneling current.¹⁹ If the defects in the barrier are paramagnetic, the exchange interaction between the defect and the tunneling electrons will result in a zero-bias conductance peak. Photoionizing the defects will remove the paramagnetism, and the zero-bias conductance peak will no longer be found. Near zero bias, the net response to light will be the sum of the increase in conductance due to the lower tunnel barrier, and a decrease in conductance because the exchange interaction has been removed.

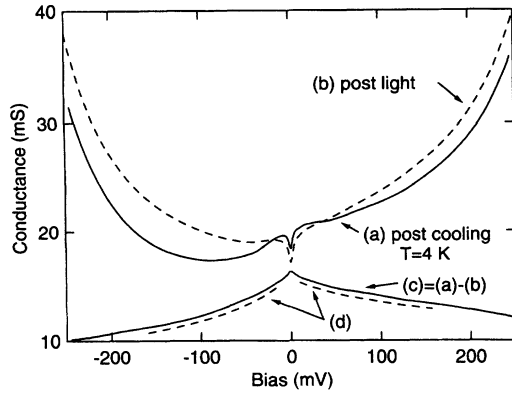


FIG. 1. The conductance $G(V)$ at 4 K: (a), after cooling in the dark. (b), after exposure to light. (c) = (a) - (b), offset vertically. (d), least squares fit of $A \ln(|V|+B)$ to (c), displaced downward from (c) for clarity.

The single barrier GaAs/Al_{0.6}Ga_{0.4}As/GaAs tunnel junctions used here were grown on n^+ -type GaAs substrates by molecular-beam epitaxy (MBE). The barriers are either 9 or 11 nm thick with the central 3 or 4 nm doped with 1×10^{18} Si cm⁻³. In one case, the central 3 nm of the barrier was doped with Be rather than Si. A 2-nm-thick undoped GaAs layer was grown on either side of the barrier for all the junctions. Further away from the barrier, the GaAs electrodes are doped with 1×10^{18} Si cm⁻³. The junctions were prepared using standard photolithography to pattern mesas with a ring-shaped top Ohmic contact to allow light into the junction.

Measurements of the bias dependence of the conductance were all carried out at 4 K in the dark using a lock-in amplifier and harmonic detection techniques. The analog electronics were calibrated by replacing the sample by a decade resistance box. The data were recorded by a computer-controlled system, which used the calibration data to convert the lock-in output to calibrated conductance data. The photoionization cross section was obtained by measuring the time

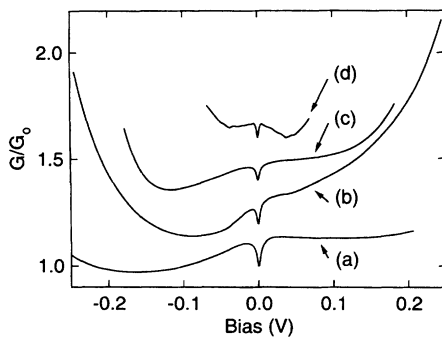


FIG. 2. The normalized conductance G/G_0 , where G_0 is the conductance at zero bias, for several samples: (a) and (b), on the same chip with a 9-nm-thick Al_{0.6}Ga_{0.4}As barrier with the central 3 nm doped with Si 1×10^{18} cm⁻³. (c), an 11-nm-thick Al_{0.6}Ga_{0.4}As barrier with the central 3 nm doped with Si 1×10^{18} cm⁻³. (d), a 9-nm-thick Al_{0.6}Ga_{0.4}As barrier with the central 3 nm doped with Be 1×10^{18} cm⁻³. Each curve has been displaced upward by 0.2 from the one below it. Curve (b) is shown in detail in Fig. 1.

dependence of the quenching of the zero-bias conductance peak, after turning on a light. A monochromator with a tungsten-halogen lamp was used as a light source to measure the spectral dependence of the quenching. The junctions were warmed to 240 K after each exposure to light to repopulate the defects in order to start each measurement with the same defect distribution. The junctions reported here were measured many times over a period of six months, and each time a junction was cooled the data were reproduced within a fraction of a percent.

The $G(V)$ measurements in Fig. 1 were made after cooling to 4 K in search of a photosensitive zero-bias conductance peak. Comparing curve (a) of Fig. 1 which was recorded after cooling, with curve (b) which was measured after shining light on the junction, demonstrates that the junctions are photosensitive. The photoinduced changes were found to persist for at least several hours by remeasuring the data several times. The approximately quadratic bias dependence found in curve (a) of Fig. 1 for $|V| > 100$ mV and in curve (b) for $|V| > 10$ mV is expected for elastic tunneling of noninteracting electrons through a trapezoidal tunnel barrier. The conductance in curve (b) of Fig. 1, for $|V| > 40$ mV, is higher than that in curve (a), which is consistent with the concept that the average barrier has been lowered by photoionizing electron traps. The conductance in curve (a) of Fig. 1 is greater than that in curve (b) for $|V| < 40$ mV, indicating the presence of a broad zero-bias conductance peak superimposed on the quadratic background. The absence of the peak in curve (b) of Fig. 1 indicates that it is due to an additional transport mechanism that is quenched by light. Both curves (a) and (b) of Fig. 1, and all the data presented in this paper contain a sharp zero-bias conductance minimum for $|V| < 10$ mV. Since no obvious changes have been observed due to shining light on the junctions, the zero-bias minima are of no interest in this paper. Almost all semiconductor tunneling data exhibit sharp zero-bias conductance depressions that have been associated with resonance tunneling via defects,¹¹ acoustic phonons,¹¹ and in one recent study with single-electron tunneling via a defect.²⁰ Conductance peaks like that in curve (a) of Fig. 1 are less common than the sharp conductance minimum. The zero-bias conductance peaks reported in the literature have been shown to be associated with tunneling via paramagnetic defects in the barrier.

The data in curve (b) of Fig. 1 were remeasured up to 15 h after shining the light on the sample, and they were found to be indistinguishable from those measured immediately after turning the light off, indicating a persistent photoeffect. A partial recovery of the data in curve (a) of Fig. 1 was observed after warming the junction to 70 K, and a recovery to within 0.5% was measured after warming to 240 K. These recovery temperatures are consistent with those measured for the DX defect after exposure to light.

The shape of the conductance peak in curve (a) of Fig. 1 was examined in more detail by subtracting curve (b) from it to produce curve (c). The exchange-interaction tunneling model predicts the bias dependence of the conductance peak is $A \ln(|V|+B)$, where A is related to the number of defects and the strength of the interaction, and B is related to phenomena that broaden the peak. The negative-bias data were fit separately from the positive-bias data, and the results are

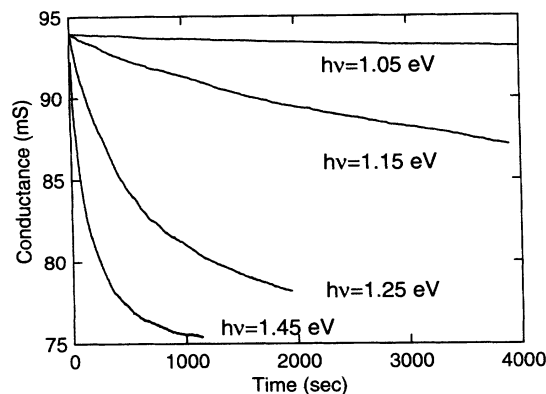


FIG. 3. The time dependence of the conductance of the junction shown in curve (a) of Fig. 2 while being exposed to light at the indicated photon energy.

the dashed curves (d), which are displaced slightly below (c) because they are indistinguishable from the data.

Zero-bias conductance peaks have been found in junctions prepared from several different MBE growths as illustrated in Fig. 2. Each curve in Fig. 2 has been normalized by its conductance at zero bias, because they vary widely in conductance due to differences in thicknesses, barrier doping, and device area. All the data shown here exhibit the photoquenching of the broad zero-bias conductance peak, the increase in conductance at high biases after exposure to light, and the persistence of the photoinduced changes. Curves (a) and (b) of Fig. 2 are from two different junctions on the same chip, and they are shown to illustrate some of the variation in shape from device to device on a given chip. The same features are found in curve (c) of Fig. 2 for a junction which has an 11-nm-thick barrier with the central 4 nm doped with 1×10^{18} Si cm $^{-3}$ compared to the devices in curves (a) and (b), which have a 9-nm-thick barrier with the central 3 nm doped with 1×10^{18} Si cm $^{-3}$. In some cases, narrower peaks with smaller amplitudes than those in curves (a), (b), and (c) of Fig. 2 have been found in junctions whose barriers were not intentionally doped with Si, such as the device shown in curve (d) of Fig. 2, which has a 9-nm-thick barrier with the central 3 nm doped with 1×10^{18} Be cm $^{-3}$. Because the exchange interaction depends upon the amplitude of the wave function of the tunneling electron at the defect in the barrier, the distribution of Si in the barrier, particularly near the GaAs/Al $_x$ Ga $_{1-x}$ As interface, is believed to play a major role in determining the width and amplitude of the conductance peak. It would not be surprising if Si from the GaAs electrodes diffused to the GaAs/Al $_x$ Ga $_{1-x}$ As interface during the MBE growth of a junction like that in curve (d) of Fig. 2.¹⁹

The time dependence of the zero-bias conductance is shown in Fig. 3 for the junction in curve (a) of Fig. 2 to illustrate the large increase in the rate at which the conductance is quenched as the photon energy is increased. A least-squares-fitting procedure was used to fit the data to the sum of two exponentials, $A_1 \exp(-t/\tau_1) + A_2 \exp(-t/\tau_2)$, to extract the time constants τ . The photoionization cross section σ_n^0 was calculated from the time constant using $\sigma_n^0 = 1/\tau\phi$, where ϕ is the photon flux. For the data in Fig. 3, the am-

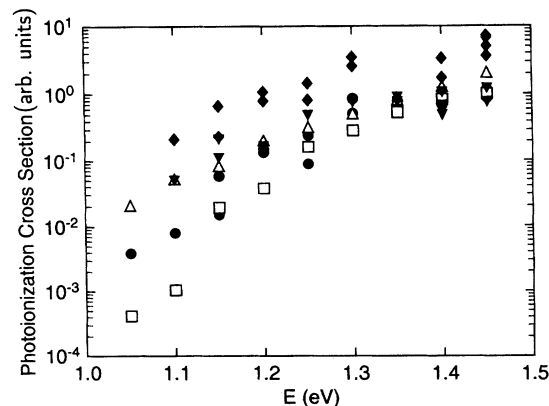


FIG. 4. A comparison of the photoionization cross sections for the junctions shown in curve (a) of Fig. 2, solid circles and diamonds, and curve (b) of Fig. 2, solid triangles with an aluminum fraction of 0.6 with that reported in the literature (Refs. 11 and 12) for aluminum fractions of 0.48 (open squares) and 0.74 (open triangles) obtained from photocapacitance measurements of Schottky barriers.

plitude of the exponential with the longer time constant is about two times larger than the amplitude of the one with the smaller time constant, and therefore represents the center with the larger concentration. Since the absolute photon flux at the junction is hard to measure, the cross sections found here have been normalized by setting the cross section at $h\nu = 1.45$ eV for the slower transient to 1.

The cross sections for both exponentials are plotted in Fig. 4 by the solid diamonds for the faster transient and solid circles for the slower one. Also shown here by the solid triangles is the photoionization cross section for the junction in curve (b) of Fig. 2, which is well fit by a single transient. The open squares and triangles in Fig. 4 are cross sections reported in the literature for aluminum fractions of 0.48 and 0.74, respectively.^{21,22} These were obtained by photocapacitance on Schottky barriers at about 80 K. The literature values were also normalized by setting the cross section for the 0.48 data at $h\nu = 1.45$ eV to 1. The slower transient, solid circles, and the solid circles for the second junction are found to compare well with the literature values for DX. The solid diamonds, which have a larger cross section than the literature data, also correspond to a defect being quenched. These data may reflect that there are different defect centers, possibly because the defects are near a GaAs/Al $_x$ Ga $_{1-x}$ As interface.

In conclusion, a conductance peak has been observed at 4 K in a number of single-barrier GaAs/Al $_x$ Ga $_{1-x}$ As/GaAs tunnel junctions. The zero-bias conductance peak is a signature that tunneling is occurring via a paramagnetic defect in the barrier. The peak is quenched by shining light on the junction, and the quenching persists for long periods of time. The spectral dependence of the normalized photoionization cross section agrees with that reported in the literature for the Si DX center in Al $_x$ Ga $_{1-x}$ As. These facts lead to the association of the conductance peak with the DX center, and since the peak is found after cooling in the dark, it is the DX in its ground state. Since the zero-bias conductance peaks

reported here involve tunneling via a paramagnetic defect in the $\text{Al}_x\text{Ga}_{1-x}\text{As}$ barrier, the results of this experiment demonstrate that paramagnetic DX centers exist in $\text{Al}_x\text{Ga}_{1-x}\text{As}$.

We would like to thank T. A. Kennedy for his useful discussions. This work was supported in part by the Office of Naval Research. The work at Howard University was supported by NSF Cooperative Agreement No. RII-8714767.

-
- ¹D. V. Lang, R. A. Logan, and M. Jaros, *Phys. Rev. B* **19**, 1015 (1979).
- ²For recent reviews of DX see DX Centers and Other Metastable Defects in Semiconductors, Mauterndorf, Austria, 1991 [*Semicond. Sci. Technol.* **B 6**, 10 (1991)]; P. M. Mooney, in *The Physics of Semiconductors*, edited by E. M. Anastassakis and J. D. Joannopoulos (World Scientific, Singapore, 1990), p. 2600.
- ³D. J. Chadi and K. J. Chang, *Phys. Rev. Lett.* **61**, 873 (1988).
- ⁴P. M. Mooney, W. Wilkening, U. Kaufmann, and T. F. Kuech, *Phys. Rev. B* **39**, 5554 (1989).
- ⁵M. Fockele, J.-M. Spaeth, H. Overhof, and P. Gibart, *Semicond. Sci. Technol.* **6**, B88 (1991).
- ⁶S. Katsumoto, N. Matsunaga, Y. Yoshida, K. Sugiyama, and S. Kobayashi, *Jpn. J. Appl. Phys.* **29**, L1572 (1990).
- ⁷K. A. Khachatryan, D. D. Awschalom, J. R. Rozen, and E. R. Weber, *Phys. Rev. Lett.* **63**, 1311 (1989).
- ⁸M. Baj, L. H. Dmowski, and T. Slupinski, *Phys. Rev. Lett.* **71**, 3529 (1993).
- ⁹J. A. Wolk, M. B. Kruger, J. N. Heyman, W. Walukiewicz, R. Jeanloz, and E. E. Haller, *Phys. Rev. Lett.* **66**, 774 (1991).
- ¹⁰L. Dobaczewski and P. Kaczor, *Phys. Rev. B* **44**, 8621 (1991).
- ¹¹For a review of zero-bias anomalies in electron tunneling, see E. L. Wolf, *Principles of Electron Tunneling Spectroscopy* (Oxford University Press, New York, 1985).
- ¹²J. Appelbaum, *Phys. Rev. Lett.* **17**, 91 (1966).
- ¹³P. W. Anderson, *Phys. Rev. Lett.* **17**, 95 (1966).
- ¹⁴J. A. Appelbaum, *Phys. Rev.* **154**, 633 (1967).
- ¹⁵P. W. Anderson, *Phys. Rev.* **124**, 41 (1961).
- ¹⁶S. Bermon, D. E. Paraskevopoulos, and P. M. Tedrow, *Phys. Rev. B* **17**, 2110 (1978).
- ¹⁷D. C. Tsui, *Solid State Commun.* **7**, 91 (1969).
- ¹⁸E. L. Wolf and D. L. Losee, *Phys. Rev. B* **2**, 3660 (1970).
- ¹⁹T. C. L. G. Sollner, H. Q. Le, C. A. Correa, and W. D. Goodhue, *Appl. Phys. Lett.* **47**, 36 (1985).
- ²⁰K. Hess, N. Holonyak, Jr., and T. A. Richard, *Appl. Phys. Lett.* **63**, 1408 (1993).
- ²¹R. Legros, P. M. Mooney, and S. L. Wright, *Phys. Rev. B* **35**, 7505 (1987).
- ²²P. M. Mooney, G. A. Northrop, T. N. Morgan, and H. G. Grimmeiss, *Phys. Rev. B* **37**, 8298 (1988).